Contents lists available at ScienceDirect

Chemical Engineering Research and Design

journal homepage: www.elsevier.com/locate/cherd

Pressurised calcination–atmospheric carbonation of limestone for cyclic CO_2 capture from flue gases

Masoud Kavosh[a], *Kumar Patchigolla*[a,*], *John E. Oakey*[b], *Edward J. Anthony*[a], *Scott Champagne*[c], *Robin Hughes*[c]

[a] *Centre for Combustion, Carbon Capture and Storage, Cranfield University, Cranfield, UK*
[b] *Centre for Power Engineering, Cranfield University, Cranfield, UK*
[c] *Natural Resources Canada, CanmetENERGY, 1 Haanel Drive, Ottawa, ON, Canada*

ARTICLE INFO

Article history:
Received 31 January 2015
Received in revised form 3 June 2015
Accepted 13 June 2015
Available online 19 June 2015

Keywords:
Pressurised calcination
Fluidised bed process
Ca looping cycles
Compression energy

ABSTRACT

A study was carried out to investigate the CO_2 capture performance of limestone under atmospheric carbonations following pressurised calcination. A series of tests was carried out to study the role of pressurised calcination using a fluidised bed reactor. In this investigation, calcination of limestone particles was carried out at three levels of pressure: 0.1 MPa, 0.5 MPa, and 1.0 MPa. After calcination, the capture performance of the calcined sorbent was tested at atmospheric pressure. As expected, the results indicate that the carbonation conversion of calcined sorbent decreases as the pressure is increased during calcination. Pressurised calcination requires higher temperatures and causes an increase in sorbent sintering, albeit that it would have the advantage of reducing equipment size as well as the compression energy necessary for CO_2 transport and storage, and an analysis has been provided to give an assessment of the potential benefits associated with such an option using process software.

1. Introduction

Current technologies for capturing CO_2 are based on absorption by means of liquid solvents, which are expensive and have serious drawbacks in terms of the energy requirements vs. solvent regeneration percentage (Feron and Hendriks, 2005). Solid sorbents offer considerable potential, especially if the sorbents are inexpensive and remain effective over many sorption/regeneration cycles. Using limestone in a Ca-looping cycle appears to be a promising approach based on the reversible calcination/carbonation reaction: $CaCO_3 \leftrightarrow CaO + CO_2$, for CO_2 capture.

During the cyclic capture of CO_2 by circulating solid sorbents transferred between the carbonation reactor (carbonator, combustor, gasifier, or steam reformer) and the calcination reactor, sorbents experience a loss in their ability to capture CO_2. The sorbent performance over many cycles is influenced by a number of factors including the total pressure, CO_2 partial pressure, temperature, sorbent composition, carbonation period, calcination conditions, and the presence or absence of other gases such as steam and SO_2 (Anthony, 2008; Sun et al., 2007a; Kavosh et al., 2014). The performance of a Ca looping system could potentially be improved by means of a pressurised system operating at 850–900 °C, which is typical of fluidised bed combustion conditions, and so far this has only been explored using a pressurised thermogravimetric analyser (PTGA) (Chen et al., 2010). Such a route might also make sense for enhanced H_2 production in a pressurised gasifier for clean energy production for instance.

However, the situation concerning pressurised calcination is less clear, and the most likely reason for carrying this out would be to reduce compression costs associated with carbon capture, since the solid sorbents carrying the CO_2 are themselves not subject to losses associated with pressure changes

* *Corresponding author.* Tel.: +44 0 1234 750111; fax: +44 0 1234 754036.
E-mail address: k.patchigolla@cranfield.ac.uk (K. Patchigolla).
http://dx.doi.org/10.1016/j.cherd.2015.06.024

Nomenclature

ASU	air separation unit
C	volume fraction of gas species
FBR	fluidised bed reactor
MFC	mass flow controller
m_0	initial sample mass [g]
M_{CaCO_3}	relative molar mass of limestone [g/mol].
P_{CO_2}	CO_2 partial pressure [MPa]
P_{eq}	equilibrium pressure [MPa]
PTGA	pressurised thermogravimetric analyser
Q	gas flow rates [L/min]
SEM	scanning electron microscopy
U	superficial velocity [m/s]
U_{mf}	minimum fluidising velocity [m/s]
$Vm_{CO_2}(T, p)$	molar volume of CO_2 at a given temperature and pressure [L/mol]
$X_{carb}(t)$	carbonation conversion at any given time

and in this case only the gases in the calciner need to be pressurised. It is also known that a lower partial pressure of CO_2 can potentially increase the calcination rate by providing a higher driving force for the removal of CO_2 from the calcined sorbent (Sakadjian et al., 2007; García-Labiano et al., 2002; Dennis and Hayhurst, 1987). Barker stated that CO_2 concentration has no influence on the calcination rate if it is well below the decomposition pressure (Barker, 1973). There appear to be considerable discrepancies in the literature on the effects of pressure on calcination. Thus, Dennis and Hayhurst (1987) found that an increase in pressure resulted in a decrease in the calcination rate, even in the absence of CO_2. Prior to this study, investigations on the effect of CO_2 partial pressure, P_{CO_2} on calcination had led to different conclusions. Several investigations considered the reaction rate as a linear function of $(P_{CO_2} - P_{eq})$ (Silcox et al., 1989; Khraisha and Dugwell, 1989; Fuertes et al., 1993). However, Khinast et al. (1996) presented an exponential decay in the calcination rate constant with P_{CO_2} Sun et al. (2007b) studied the effect of pressurised calcination and carbonation on the cyclic sorption process using PTGA and found that pressurised calcination with no CO_2 present did not affect sorbent reversibility. However, there is no information on the cyclic CO_2 capture ability of sorbents involving pressurised calcination. Moreover, the majority of studies have been based on TGA experiments, with the limitations that this implies in terms of small sample sizes, making solid characterisation impossible, and a lack of the hydrodynamic phenomena associated with carbon capture in a fluidised bed combustor (Liu et al., 2000). Pressurised calcination results in a high-pressure CO_2 stream at the output of the calciner, and hence reduces the energy required for the compression stage. In addition, steam condensation will occur at higher temperatures for a potential increase in overall efficiency if this heat can be recuperated. Further, calcination under higher pressure requires a smaller reactor, hence, lower fixed costs. Therefore, process intensification is a potential advantage of pressurised calcination. It might also offer potential in terms of "smoother" operation at high pressures with smaller bubbles and higher dense phase voidage in the fluidised bed reactor (FBR), leading to better contact between particles and the gas and enhanced heat and mass transfer, when using higher oxygen levels in the calciner (Sanchez-Biezma, 2014) with the goal of reducing the size of the calciner.

To explore the potential of this approach an experimental study was carried out on the performance of limestone in a cycle which included pressurised calcination. This was supplemented by a UniSim process simulation to evaluate the change in required compression energy with the calciner operating at different pressures. The simulation looks at all critical elements of the plant and also includes an estimate of the air separation unit (ASU) energy consumption given the oxygen flowrate and delivery pressure required for the calciner using a correlation from literature (Fu and Gundersen, 2012) and the same pressures used for the test regime, namely 0.1, 0.5 and 1.0 MPa.

2. Experimental equipment and methodology

A small bubbling fluidised bed was designed, capable of operating at temperatures up to 1200 °C. A schematic of the system is presented in Fig. 1. The major components consist of a quartz tube, an outer tube and an electrical heater. This is followed by a hot gas filter for the flue stream, a gas dryer, a water pump, and an ADC 7000 gas-analyser unit to measure CO_2 concentration. The outer tube has a height of 1180 mm and internal diameter of 37 mm. The distributor consists of a sintered plate, with a preheater section at the base to achieve the desired reaction temperature.

Reactor temperatures were measured by a K-type thermocouple, and they and the differential pressure across the bed were recorded by a data acquisition system. Reactant gases, CO_2, O_2, and N_2, were fed to the system via a bottom flange of the outer tube, and passed through the pre-heater zone prior to entering the reactor. The flow rates of gases were controlled using highly accurate Mass Flow Controllers (MFC), (Bronkhorst; EL-FLOW Series).

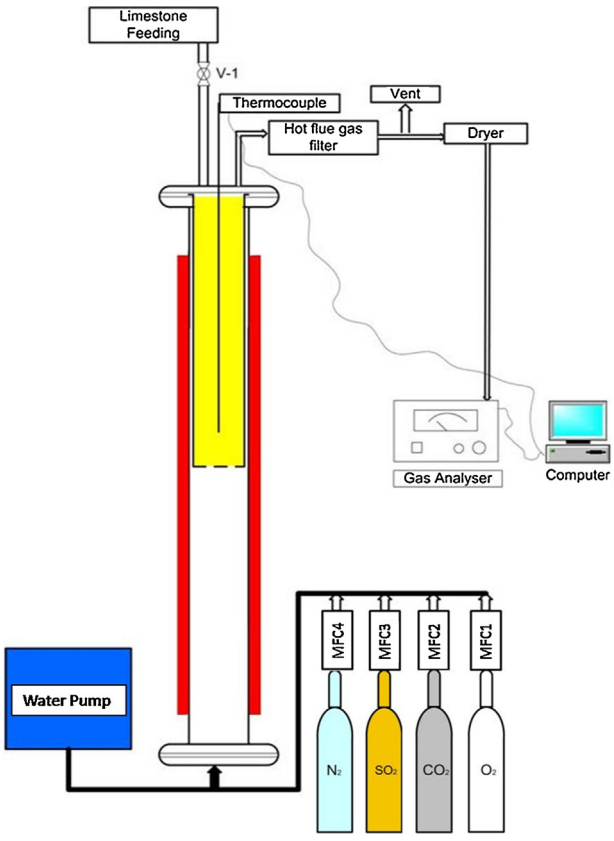

Fig. 1 – Bubbling bed test facility.

Table 1 – Experimental conditions in tests run with pressurised calcination and atmospheric carbonation.

Test run (pressure during calcination)	CO_2 partial pressure in calciner* (MPa)
Press 1 (0.1 MPa)	0.015
Press 2 (0.5 MPa)	0.075
Press 3 (1.0 MPa)	0.15

* All mixtures in calciner and carbonator are 15% CO_2 + 4% O_2 + N_2 balance.

For this work the limestone used was Longcliffe (Longcal SP52), which has a minimum 98.25% $CaCO_3$ content, and specific gravity 2.65 g/cm^3. The limestone particles were ground and sieved to 125–250 μm for the experiments presented in this article. The chemical composition of the limestone used has been presented elsewhere (Kavosh et al., 2014). The multi-cycle split calcination and carbonation experiments with elevated pressure during the sorbent decomposition stages were carried out in a bubbling fluidised bed reactor. The tests were run in batch mode.

The steel reactor was loaded with 10 g of limestone and then heated for the calcination. In order to reduce the reaction period and to prevent subsequent challenges in the steel reactor (such as sintering of particles and corrosion of the reactor), the pressurised test at 1.0 MPa was carried out using 5 g of sample. The temperature of the fluidised bed reactor was raised at the rate of 25 °C/min to the target value of 950 °C. The reactor bed was fluidised with a sweep gas at flow rates of 1.2, 6.0, and 12.0 NL/min to provide a bubbling regime during the gas–solid reaction under elevated pressures. The calcination step was carried out until CO_2 levels had dropped to a negligible level. After the calcination the reactor was cooled to 650 °C at the rate of 10 °C/min, and the pressure was reduced to atmospheric level.

Once the temperature reached 650 °C, the produced lime was exposed to carbonating gas mixtures containing a certain percentage of CO_2 (15%) at a flow of 1.6 NL/min. The carbonation step was continued until the reaction was completed, which corresponded to CO_2 vol. % reaching a constant level in the exit gas stream effectively equal to the feed level. The capture step lasted about 30 min. After complete carbonation, the bed temperature was increased again to 950 °C to regenerate the lime. These sequential processes were repeated for 8–10 cycles for each set of operating pressures and the experimental conditions for both calcination and carbonation are given in Table 1. Typically, the unit was run at a U/U_{mf} ratio of about 3 to 4.

The changes in sorbent morphology and microstructure of calcined particles after the first and final cycles were investigated using scanning electron microscopy (SEM). The specific surface area, pore volume, porosity, and pore size distribution of the CaO particles were also determined. More details of the instruments and methods used for morphological measurements of particles are presented elsewhere (Kavosh et al., 2014). Finally, it is recognised that the heating rates achieved in this system are far slower than particles would experience in a real system, and if sintering is excessive under these conditions, then it is anticipated that it would be much worse in a real system, in which case high-pressure calcination is likely to be problematic if the results are negative in this type of system (German, 1996).

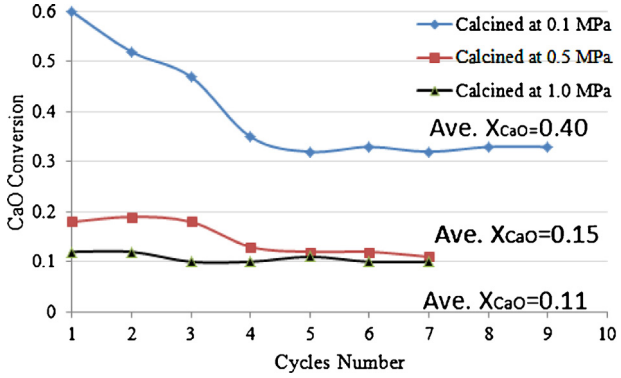

Fig. 2 – Carbonation conversion curves of calcined samples produced at elevated pressure and carbonated at atmospheric pressure. Calcination: at 950 °C, in 15% CO_2, 3% O_2 and N_2 balance. Carbonation: at 650 °C, in 15% CO_2, 4% O_2 and N_2 balance.

3. Results and discussions

Carbonation conversions of the calcined particles were calculated by integrating the CO_2 concentration over the reaction time using the following equation (Kavosh et al., 2014):

$$X_{Carb}(t) = \frac{Q_{in} M_{CaCO_3}}{m_0 V_{mCO_2}(T,p)} \int_0^t \frac{C_{CO_2\ in} - C_{CO_2\ out}(t)}{1 - C_{CO_2\ out}(t)} dt \quad (1)$$

where $X_{carb}(t)$ is the carbonation conversion at any given time, Q denotes gas flow rates [L/min], C shows volume fractions of gas species, $Vm_{CO}(T, p)$ is the molar volume of CO_2 at a given temperature and pressure [L/mol], m_0 denotes the initial sample mass [g] and M_{CaCO_3} is the relative molar mass of limestone [g/mol].

The carbonation conversion curves obtained are shown in Fig. 2. As can be seen, the carbonation conversion of calcined sorbent decreases as the pressure is increased during calcination. The average conversion for the CaO produced at atmospheric pressure adopted the rather high value of 0.40; however, it declined significantly to 0.15 and 0.11 for the sorbents calcined under 0.5 MPa and 1.0 MPa, respectively. What is noticeable is a dramatic difference between 0.1 MPa and 0.5 MPa, and relatively small change between 0.5 and 1 MPa.

Fig. 3 shows that the decomposition began at 790 °C, 870 °C and 940 °C at elevated pressures of 0.1 MPa, 0.5 MPa, and 1.0 MPa, respectively.

The time required for calcination increased significantly with increasing pressure. The calcination periods were 13 min, 40 min, and 110 min for calcination at 0.1 MPa, 0.5 MPa, and 1.0 MPa pressure, respectively, as expected (Sun et al., 2007b; Hughes et al., 2009; Stanmore and Gilot, 2005; Abanades et al., 2005). These results were supported by the SEM images of sorbents after the first and the last cycle of calcination at elevated pressure, Fig. 4. The number of cycles and the calcination pressures are given on each SEM image. Fig. 4a shows the porous structure of particles calcined at 0.1 MPa, with a desirable sorbent texture consisting mainly of small pores. Existence of small pores increases the surface area and enables sorbents to achieve a higher CO_2 capture. The series of images shown in Fig. 4a to f illustrates the trend of surface texture of sorbents with increasing calcination pressure and number of cycles. The images reveal the development of necks between the

Table 2 – Porous structural properties of calcined particles at elevated pressure after the initial and multiple cycles (see Table 1 for details of reaction conditions).

Calcined sample, pressure and cycle number	S_{BET} (m^2/g)	Pore volume (cm^3/g)	Calcined sample pressure and cycle number	S_{BET} (m^2/g)	Pore volume (cm^3/g)
0.1 MPa, 1st cycle	18	0.022	0.1 MPa, 10th cycle	5.7	0.010
0.5 MPa, 1st cycle	2.5	0.004	0.5 MPa, 8th cycle	1.2	0.002
1.0 MPa, 1st cycle	1.1	0.001	1.0 MPa, 8th cycle	0.25	0.0006

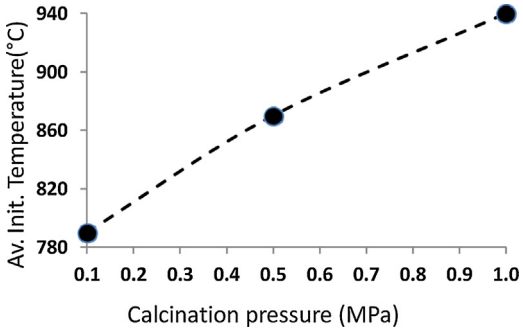

Fig. 3 – Effect of pressure on the incipient bed temperature for calcination.

grains and increasing pore size (associated with sintering).

The specific surface area and pore volume of particles are given in Table 2. Pore volumes show the volumes of small pores and medium-size pores (~60–300 nm). The values are calculated as the difference between cumulative volume of pores with diameters of 1.7–300 nm, and the pore volume measured for smaller pores. Table 2 gives the BET specific surface areas that were measured at 18 m^2/g for the initial calcined sorbent at 0.1 MPa pressure, and that value decreased to 2.5 and 1.1 m^2/g for calcined particles produced at pressures of 0.5 and 1.0 MPa, respectively. The corresponding volumes of small pores were 0.022, 0.004, and 0.001 cm^3/g for particles calcined at three levels of the calcination pressures.

Pore size distributions, plotted in Fig. 5, reveal that the number of small pores is higher in CaO particles, which were calcined at 0.1 MPa and that increasing pressure dramatically decreases the number of those pores even by the first cycle. It is also clear that even by the 10th cycle calcined particles have more pores in the range of 10 to 100 nm than do ones calcined at elevated pressure by the first cycle (Fig. 5).

Specific surface areas and meso-pore volumes for CaO particles calcined in the 10th or 8th cycle are given in Table 2. The surface areas and pore volumes of calcined sorbent decreased after pressurised calcination. Calcined sorbent produced under 0.1 MPa (in the 10th cycle) contains a surface area of 5.7 m^2/g, and pore volume of 0.01 cm^3/g. However, the corresponding values for CaO calcined under 0.5 MPa and 1.0 MPa (in the 8th cycle) have decreased to 1.2 and 0.25 m^2/g with surface area, and 0.002 and 0.0006 cm^3/g of pore volume, respectively. There also seems little doubt that sorbent deterioration would have been worse if the calcination gases had been nearly pure CO_2. Given the significant fall in sorbent carrying capacity, it seems likely that such a system would also require some reactivation strategy, such as for instance by hydration (Manovic and Anthony, 2007) using a separate reactor, or by using high CO_2 concentrations to reactivate the sorbent after calcination, as suggested by CanmetENERGY and the Spanish Research Council, and now being developed by the Spanish Research Council (Elena Diego et al., 2014; Salvador et al., 2003). Although such options increase complexity and cost, they may well be necessary in the future if Ca looping technology is to be considered fully competitive with amine scrubbing in situations where there is not a major demand for the spent sorbent such as the cement industry. However, a detailed analysis of the use of reactivation strategies is outside the scope of this paper.

4. Simulation of pressurised calcination

The steady-state simulation is based on a typical retrofit case where a calcium looping system is integrated into an existing plant. In this case, a 250 MW_{th} air-fired coal boiler is the CO_2 source of interest. The key assumptions for this simulation are that the carbonator is operated at atmospheric pressure and 650 °C as would be expected if the Ca looping plant were added to an existing plant. The calciner is operated at 0.1, 0.5 and 1.0 MPa in different cases to determine the impact of calciner operating pressure on the required energy to produce a 15.0 MPa pipeline-ready CO_2 stream. For the purposes of the simulation we assumed that the fuel used in the base plant and calciner was Daw Mills coal (see Table 3), and we have ignored sulphur removal assuming that inherent capture of SO_2 is essentially 100% (Arias et al., 2013). A simplified process flow diagram of the simulated process is shown in Fig. 6. The significant assumptions on which the simulation is based are presented in Table 4 and the composition of the inlet stream to both the calciner and carbonator reactors are presented in Table 5. The temperature of the calciner was selected based on the partial pressure of CO_2 present and the equilibrium relationship presented by García-Labiano et al. (2002) The calciner temperature must increase as the absolute pressure increases due to the inherent increase in the partial pressure of CO_2. In addition to those assumptions, it should be noted that no heat integration has been performed. All heating and cooling are done with heater or cooler units. These units will only

Table 3 – Daw Mill coal properties.

Proximate analysis	Daw Mill coal		
	Ar	Dry	Daf
Moisture (wt%)	3.2		
Ash (wt%)	12.39	12.8	
Volatile matter (wt%)	27.59	28.5	32.68
Fixed carbon (wt%)	56.82	58.7	67.32
Ultimate analysis			
Carbon (wt%)	67.08	69.3	79.47
Hydrogen (wt%)	4.16	4.3	4.93
Nitrogen (wt%)	1.16	1.2	1.38
Sulphur (wt%)	1.43	1.48	1.7
Oxygen (wt%)	10.32	10.66	12.22
Gross CV (MJ/kg)	26.29	27.16	31.14
Net CV (MJ/kg)	25.3	26.22	30.07

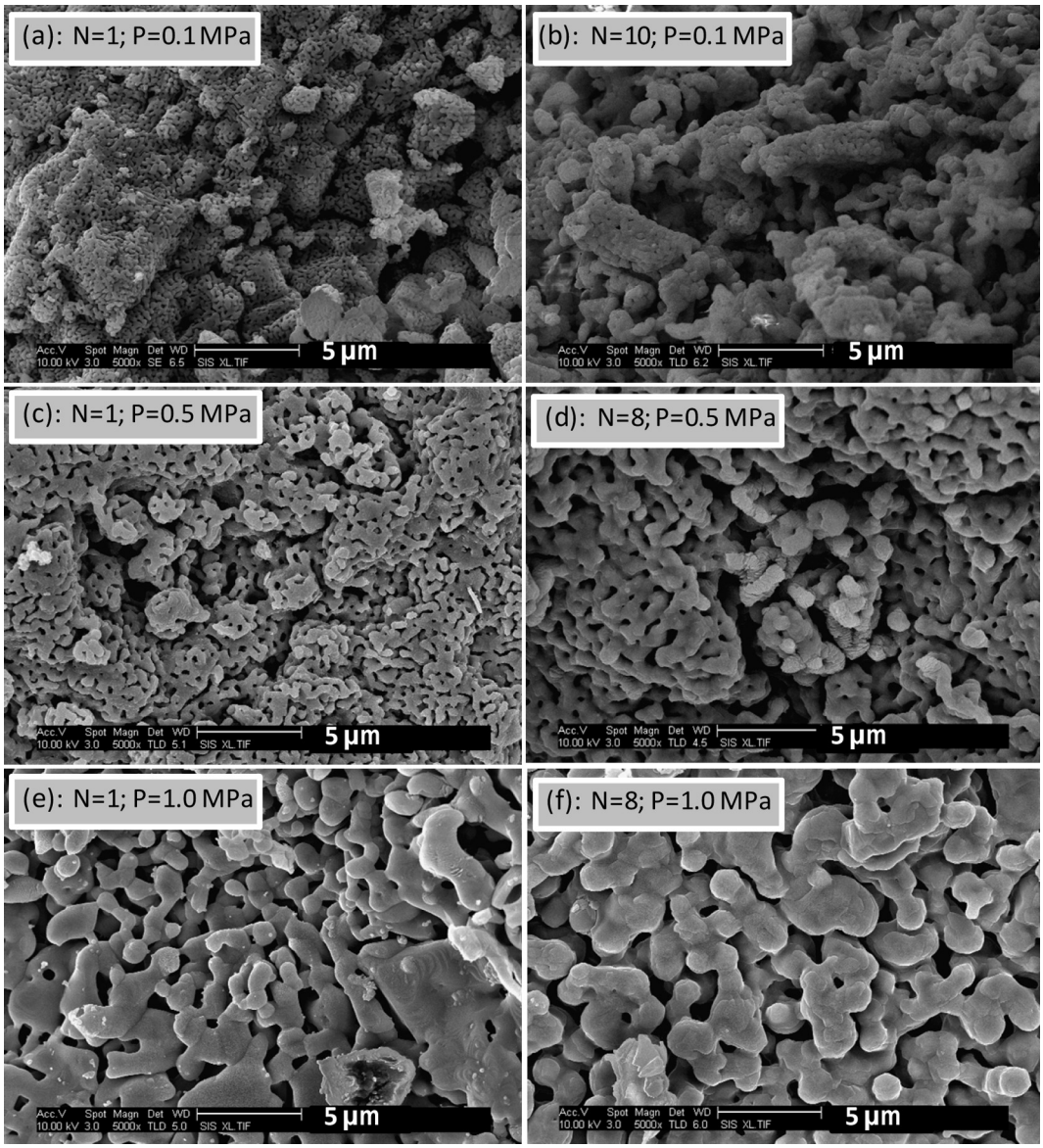

Fig. 4 – SEM images of the calcined particles produced at elevated pressure, after one and eight cycles of calcination–carbonation. Calcinations: 15% CO_2, 3% O_2 and N_2 balance; carbonation was carried out with a gas composition of 15% CO_2, 4% O_2 and N_2 balance.

calculate the amount of energy required to heat or cool the stream, not utility requirements.

Several important trends came out of the process simulation. The number of compression stages and compressor power required for each stage is summarised for three calciner operating pressures in Fig. 7. The energy required for the first compression stage is similar for all three calciner pressures. However, as the number of stages increases, there is a clear increase in required compressor power with decreasing calciner pressure. Additionally, the number of stages required

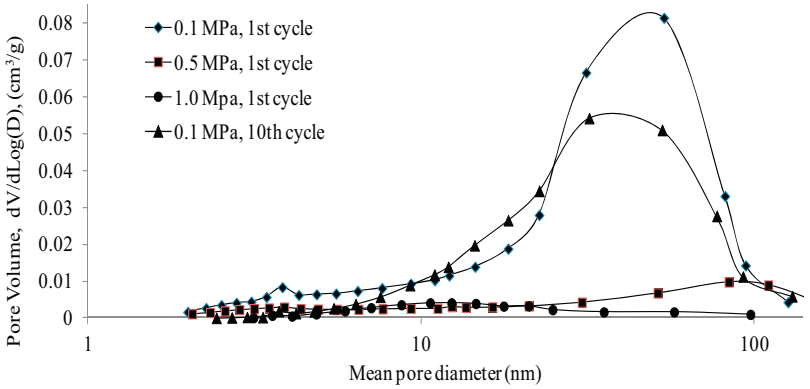

Fig. 5 – Pore-size distribution of CaO particles produced at elevated pressure (up to 1 MPa).

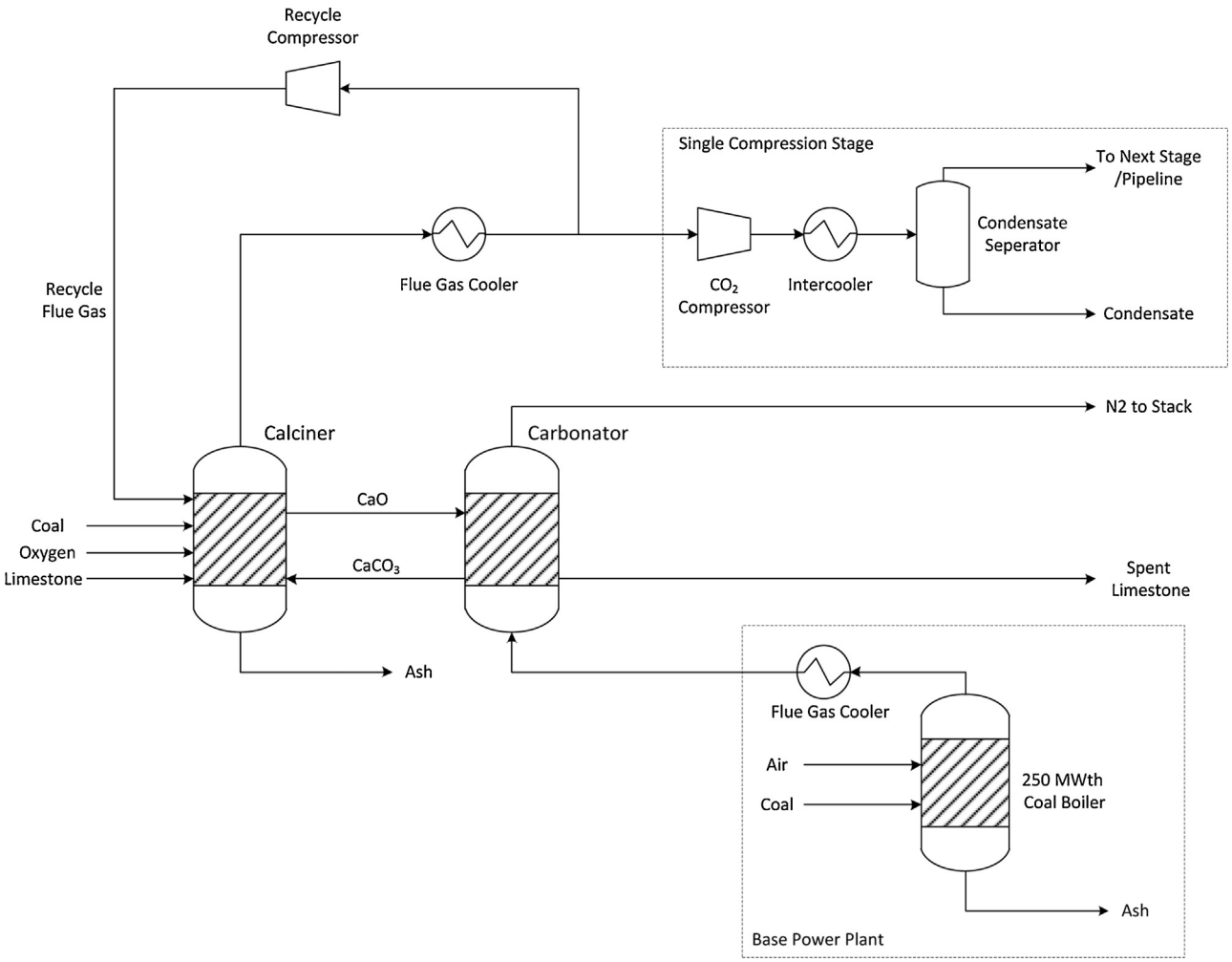

Fig. 6 – Simplified process flow diagram of UniSim simulation.

Table 4 – Key assumptions made in the development of the UniSim process simulation.

Calciner	Carbonator	CO_2 compression	Base boiler (CO_2 source)
Operated at 897 °C, 987 °C and 1040 °C 0.1, 0.5 and 1.0 MPa absolute pressures Oxy-fuel combustion with flue gas recycle Complete combustion of coal Equilibrium reactor used for calcination Solids enter from carbonator at 650 °C Flue gas cooled to 130 °C	Operated at 650 °C Atmospheric pressure Solids from calciner enter at 750 °C 20% carbonation conversion 90% capture efficiency Exhaust cooled to 150 °C	Pipeline pressure of 15.0 MPa Maximum compression ratio of 2.5 Cooled to 35 °C between stages 75% polytropic efficiency for compressors	250 MW_{th} air-fired boiler Flue gas cooled to 200 °C before carbonator

to compress the CO_2 to 15.0 MPa in the 0.1 MPa case is double that of the 1.0 MPa case. The simulation results indicate that there is an opportunity to reduce both the number of compression stages required and the energy required by relatively small increases in calciner operating pressure. Although there are benefits to running at elevated pressure on the product compression side, there is a cost on the reactant side. Operating an air separation unit at the higher pressures required for pressurised calcination comes at an energy cost. ASU energy consumption was estimated using the pressure and flowrate from the simulation and a correlation from Fu and Gundersen (2012). The energy requirements for compression, intercooling and the ASU are summarised in Table 6. The increase in ASU energy consumption is greater than the reduction in required compression energy due to the increased oxygen demand driven by the higher calcination temperatures required with high CO_2 partial pressures. Comparing the 0.1 and 1 MPa cases, there is a net increase of 6.95 MW considering

Table 5 – Composition of inlet gas to the calciner and carbonator reactor from UniSim process simulation.

Component (mol%)	Calciner gas inlet	Carbonator gas inlet
CO_2	0.68	0.13
O_2	0.02	0.05
N_2	0.04	0.75
H_2O	0.26	0.07

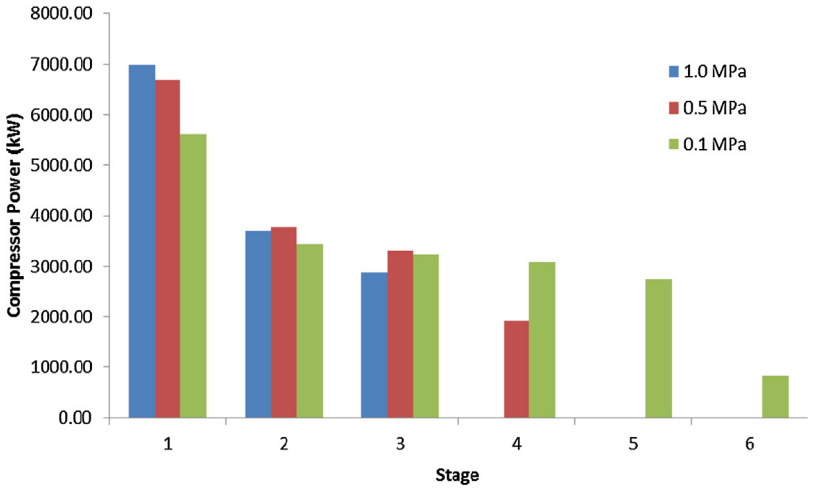

Fig. 7 – Compressor power needed for each stage for the calciner operating at 0.1, 0.5 and 1.0 MPa.

Table 6 – Total compression, intercooling and air separation unit duties for process simulation cases with the calciner operating at 0.1, 0.5 and 1.0 MPa.

Calciner operating pressure (MPa)	Calciner temperature (°C)	CO_2 partial pressure in Calciner (MPa)	Total compression duty (MW)	Total intercooling duty (MW)	Air separation unit duty (MW)
0.1	897	0.07	18.97	44.17	15.00
0.5	987	0.36	15.68	46.77	21.87
1.0	1040	0.71	13.56	46.50	25.02

only compression, intercooling and ASU duties. The reduction in compression energy demand is approximately half of the increase in ASU demand. This indicates there could be a net increase in energy usage in a calcium looping plant operating with a pressurised calciner.

There are additional potential drawbacks to operating a calcium looping plant with a pressurised calciner and atmospheric carbonator. Pressure-swing equipment, such as lock hoppers, is generally not designed to function at temperatures as high as 950 °C. There would likely be a need to cool the solids after exiting the calciner or carbonator before the pressure-swing equipment. This could result in a significant energy penalty as the sorbent carries a large amount of heat between the two fluid beds. This loss of heat would have to be well integrated into the system to mitigate this, but this is likely to be the case for any pressure-swing system that can be considered.

5. Conclusions

A study was carried out on the CO_2 capture performance of limestone following pressurised calcinations and has led to the following conclusions:

Carbonation conversion of calcined sorbent decreases as the system pressure is increased during calcination. As demanded by thermodynamics the incipient temperature of calcination increases with increasing CO_2 partial pressure, but there is dramatic reduction in carbon capture for calcination with increasing CO_2 levels in the calciner, for absolute pressures between 0.1 MPa and 0.5 MPa, and a relatively small change between 0.5 and 1 MPa. In addition, as expected pressurised calcination requires higher temperatures and longer calcination times, and causes an increase in sorbent sintering, as is shown by the fact that SEM images reveal the development of necks between the grains and increasing pore size with increasing pressure during calcination. This is also reflected in the fact that the BET specific surface areas were measured for the initial calcined particles and showed a decrease for particles calcined at 0.5 and 1.0 MPa. The corresponding pore volumes experienced an extreme drop with increasing calcination pressure. While there appears to be significant plant flowsheet simplification (capital savings), a simulation performed on this system showed there is no saving in energy if a pressurised calciner is used.

Acknowledgement

The authors wish to acknowledge the Energy Theme at Cranfield University and the Engineering and Physical Sciences Research Council (EPSRC grant no: EP/G06279X/1) for financial support of the project.

References

Abanades, J.C., Anthony, E.J., Wang, J., Oakey, J.E., 2005. Environ. Sci. Technol. 39, 2861–2866.
Anthony, E.J., 2008. Ind. Eng. Chem. Res. 47, 1747–1754.
Arias, B., Diego, M.E., Abanades, J.C., Lorenzo, M., Diaz, L., Martinez, D., Alvarez, J., Sanchez-Biezma, A., 2013. Int. J. Greenhouse Gas Control 18, 237–245.
Barker, R., 1973. J. Appl. Chem. Biotechnol. 23, 733–742.
Chen, H., Zhao, C., Li, Y., Chen, X., 2010. Energy Fuels 24, 5751–5756.
Dennis, J.S., Hayhurst, A.N., 1987. Chem. Eng. Sci. 42, 2361–2372.
Elena Diego, M., Arias, B., Grasa, G., Carlos Abanades, J., 2014. Ind. Eng. Chem. Res. 53, 10059–10071.
Feron, P.H.M., Hendriks, C.A., 2005. Oil Gas Sci. Technol. 60, 451–459.
Fu, C., Gundersen, T., 2012. Energy 44, 60–68.
Fuertes, A.B., Marban, G., Rubiera, F., 1993. Chem. Eng. Res. Des. 71, 421–428.
García-Labiano, F., Abad, A., de Diego, L.F., Gayán, P., Adánez, J., 2002. Chem. Eng. Sci. 57, 2381–2393.

German, R.M., 1996. Sintering Theory and Practise. Wiley-Interscience, John Wiley & Sons.
Hughes, R.W., Macchi, A., Lu, D.Y., Anthony, E.J., 2009. Chem. Eng. Technol. 32, 425–434.
Kavosh, M., Patchigolla, K., Anthony, E.J., Oakey, J.E., 2014. Appl. Energy 131, 499–507.
Khinast, J., Krammer, G.F., Brunner, C., Staudinger, G., 1996. Chem. Eng. Sci. 51, 623–634.
Khraisha, Y.H., Dugwell, D.R., 1989. Chem. Eng. Res. Des. 67, 52–57.
Liu, H., Katagiri, S., Kaneko, U., Okazaki, K., 2000. Fuel 79, 945–953.
Manovic, V., Anthony, E.J., 2007. Environ. Sci. Technol. 41, 1420–1425.
Sakadjian, B.B., Iyer, M.V., Gupta, H., Fan, L., 2007. Ind. Eng. Chem. Res. 46, 35–42.
Salvador, C., Lu, D., Anthony, E., Abanades, J., 2003. Chem. Eng. J. 96, 187–195.
Sanchez-Biezma, A., 2014. RFCS Project 01/06/2014, 630785.
Silcox, G.D., Kramlich, J.C., Pershing, D.W., 1989. Ind. Eng. Chem. Res. 28, 155–160.
Stanmore, B.R., Gilot, P., 2005. Fuel Process. Technol. 86, 1707–1743.
Sun, P., Grace, J.R., Lim, C.J., Anthony, E.J., 2007a. Energy Fuels 21, 163–170.
Sun, P., Grace, J.R., Lim, C.J., Anthony, E.J., 2007b. AIChE J. 53, 2432–2442.